growth rate of modes in the direction of the current is most strongly affected by the change in f_e, oblique modes are more pronounced.

To compare these results with the behavior of a one-dimensional plasma the same run as shown in Figs. 1(a) and 1(b) was performed for a one-dimensional system. Here the saturation field energy is found to be much smaller than in the corresponding two-dimensional case, and so is the *average* field $E_0 = \nu_{\text{eff}}/\omega_{pe}$ plotted in Fig. 1(c). This is because in a one-dimensional system the ion sound instability is switched off by formation of a small plateau in f_e, since only a few electrons are resonant. In the two-dimensional case where a broad spectrum in θ is excited, a "plateau" cannot stabilize oblique modes—the change of f_e actually taking place is illustrated in Fig. 2—which makes the ion-sound instability more effective.

Finally, we compare the results of our two-dimensional computations with experimental values of the turbulent resistivity. Since we adopted periodic boundary conditions, the comparison has to be made with toroidal experiments. For instance, Hamberger and Jancarik[5] obtain $\nu_{\text{eff}}/\omega_{pe} \simeq (1/2\pi)(m_e/m_i)^{1/3}$ for the Buneman instability and typically a factor of 5 less in the ion-sound regime with $v_d \simeq 0.2 v_{\text{th},e}$.

Assuming $\nu_{\text{eff}} \sim v_d/v_{\text{th},e}$, we can extrapolate this result to the regime of the computer experiments, $v_d \simeq v_{\text{th},e}/2$, obtaining $\nu_{\text{eff}}/\omega_{pe} \simeq 0.007$ for $m_i/m_e = 1600$. This value is larger by a factor of 4 than the numerical result given in Table I.

The discrepancy seems to be due to the two-dimensional character of the computations, where a large "runaway" contribution reduces the effective drift of the bulk, v_{bulk}, considerably. We expect on simple geometrical grounds that in a fully three-dimensional computer experiment the number of runaway electrons will be appreciably smaller.

By way of summary, the two-dimensional computations have shown that the ion-sound instability for $v_d < v_{\text{th},e}$ can produce an effective turbulent resistivity. Saturation of the instability is achieved by ion trapping, which cannot be described adequately by any weak-turbulence approach. The relaxation of the electron distribution gives rise to a dependence of ν_{eff} on m_i/m_e, which, however, is weaker than the dependence obtained from the *ad hoc* argument $\nu_{\text{eff}} \sim \gamma_L \sim (m_e/m_i)^{1/2}$. The numerical value of ν_{eff} is smaller than that found in real experiments, which might be a result of the two-dimensional nature of the computed plasma.

The authors would like to thank Dr. K. U. von Hagenow for his help in preparing the numerical code and Dr. C. Dum for valuable discussions.

[1]J. P. Boris, J. M. Dawson, J. H. Orens, and K. V. Roberts, Phys. Rev. Lett. 25, 706 (1970).

[2]R. L. Morse and C. W. Nielson, Phys. Rev. Lett. 26, 3 (1971).

[3]C. K. Birdsall and D. Fuss, J. Comput. Phys. 3, 494 (1969).

[4]R. L. Morse and C. W. Nielson, Phys. Fluids 12, 2418 (1969).

[5]S. M. Hamberger and J. Jancarik, Phys. Rev. Lett. 25, 999 (1970).

Correlation Range and Compressibility of Xenon near the Critical Point*

I. W. Smith,† M. Giglio,‡ and G. B. Benedek

Center for Materials Sciences and Engineering, Massachusetts Institute of Technology, Cambridge, Massachusetts 02139

(Received 1 October 1971)

From the magnitude and angular dependence of the intensity of light scattered from xenon near its critical point we have measured the Ornstein-Zernike long-range correlation length ξ and the reduced compressibility $(\partial\rho/\partial\mu)_T$. We find $\xi = (3.0 \pm 0.10)\epsilon^{-0.58 \pm 0.05}$ Å and $(\partial\rho/\partial\mu)_T = (1.43 \pm 0.06) \times 10^{-9}\epsilon^{-1.21 \pm 0.03}$ g^2/erg cm^3 along the critical isochore, and $(\partial\rho/\partial\mu)_T = (0.346 \pm 0.01) \times 10^{-9}\epsilon^{-1.21 \pm 0.02}$ g^2/erg cm^3 along the coexistence curve, with $\epsilon \equiv |T - T_c|/T_c$. Using our results, we have compared the predictions of the Kawasaki-Kadanoff-Swift mode-mode coupling theories with measurements of the thermal diffusivity in xenon.

Using essentially the apparatus of Giglio,[1] we have measured the absolute magnitude and angular anisotropy of the intensity of light scattered from xenon near its critical point. The light-scattering cell is of beryllium copper with a hollow, cylindrical, optical-quality glass window

(dimensions 0.250 in. i.d., 0.750 in. o.d., and 0.625 in. high) held with its axis vertical and coincident with the axis of rotation of a rotating arm carrying the collecting optics. A horizontal 1-mW beam of 6328-Å light from a Spectra-Physics model 131 helium-neon laser is focused through the window into the xenon in the center of the window by input optics with $f/D \sim 30$. Light scattered from thermal fluctuations in the density is allowed to fall upon the photocathode of an RCA 7265 photomultiplier by collecting optics. The scattering region (that part of the focused laser beam perpendicular to and passing through the axis of the window) is imaged onto slits which define its length (which was always less than one sixth of the window inside diameter) and its height.

Only light scattered into a constant solid angle of 1.6×10^{-3} sr around the scattering angle θ was accepted. The optics were aligned at $T = 21.7$°C where the anisotropy is essentially zero. The light intensity scattered in a horizontal plane at seven angles θ was measured, and the transmitted beam power was determined by inserting calibrated attenuating filters before the photomultiplier and setting the arm at 0°. For $0°C < (T - T_c) < 0.045$°C, gravitationally induced density gradients in the xenon bent the transmitted beam down so that its intensity could not be reliably measured. By measuring the intensity of light scattered into the collection optics from points above and below the beam, we were able to remove the effect of stray light. This correction was never larger than 5% of the intensity scattered from the main beam. The laser power was electronically stabilized to 0.1%; the temperature was controlled to ±0.002°C by a two-stage servo consisting of an outer copper can with temperature-controlled water circulating through it and an inner insulated enclosure with an electronically controlled thermoelectric heat pump.

The critical temperature T_c of 16.586 ± 0.002°C was established by observing the disappearance of the phase boundary and from power-law fits of the measured divergence in $(\partial\rho/\partial\mu)_T$ and ξ. By means of a stainless-steel bellows at the bottom of the sample cell, the average density of the fluid was adjusted to be equal to the critical density to ±0.1% as determined from observations of the height of the phase boundary as a function of temperature for $T < T_c$. Above T_c all measurements of intensity were taken at the height of disappearance of the phase boundary, except in the region very close to T_c ($0.022°C \leq T - T_c \leq 0.075$ °C), where the position chosen was that for which the correlation range ξ was maximized. Below T_c the data were taken within 0.010 in. of the phase boundary. Calculations of the density variation with height using the Schofield-Litster-Ho equation of state[2] indicate that this displacement gives negligible error in the determination of ξ and $(\partial\rho/\partial\mu)_T$.

At each temperature the intensities were fit by the Einstein-Ornstein-Zernike[3,4] formula

$$\frac{P_I}{P_S} = \frac{\lambda_0^4}{k_B T \pi^2 (\partial n^2/\partial\rho)_T^2 L\Omega} \frac{1+q^2\xi^2}{(\partial\rho/\partial\mu)_T}. \quad (1)$$

In this equation P_I is the total power incident on the scattering region and P_S is total power scattered into a small solid angle Ω centered about the scattering angle θ; λ_0 is the vacuum wavelength of light, n the refractive index, ρ the mass density, and $q = (4\pi n/\lambda_0)\sin\frac{1}{2}\theta$. $(\partial\rho/\partial\mu)_T$ is the reduced compressibility, μ being the chemical potential, and ξ is the Ornstein-Zernike long-range correlation length. The scattered and transmitted beams suffer losses due to attenuation in the xenon and reflections at the surfaces of the window, but because of the cylindrical geometry these losses are exactly identical and cancel in the ratio P_{SM}/P_T of measured scattered power to transmitted power; thus $P_{SM}/P_T = P_S/P_I$. L is the length of the scattering region as seen by the collecting optics and is inversely proportional to $\sin\theta$ because the collecting optics hold constant the length of the projection of the scattering region in a plane normal to the observation direction. The index of refraction is taken from the Lorentz-Lorenz relation $(n^2-1)/(n^2+2) = K\rho$, which has been verified in the critical region; the constant $K = 0.07986$ cm^3/g, evaluated by Chapman, Finnimore, and Smith.[5]

Using Eq. (1), our measurements of P_I/P_S, L, and Ω, and the Lorentz-Lorenz formula, we were able to determine ξ and $(\partial\rho/\partial\mu)_T$ from the slope and the intercept (at $q^2 = 0$), respectively, of a computer fit to a linear variation of P_S/P_I with q^2. In Fig. 1 we show our results for $(\partial\rho/\partial\mu)_T$ both along the critical isochore and along the coexistence curve. These data can be fitted, using $T_c = 16.586$°C, by the formulas

$$(\partial\rho/\partial\mu)_{T+} = (1.43\pm0.06)\times10^{-9}\epsilon^{-1.21\pm0.03} \text{ g}^2/\text{erg cm}^3 \quad (2)$$

along the critical isochore in the temperature range $0.045°C \leq T - T_c \leq 5.1$°C, and

$$(\partial\rho/\partial\mu)_{T-} = (0.346\pm0.01)\times10^{-9}\epsilon^{-1.21\pm0.02} \text{ g}^2/\text{erg cm}^3 \quad (3)$$

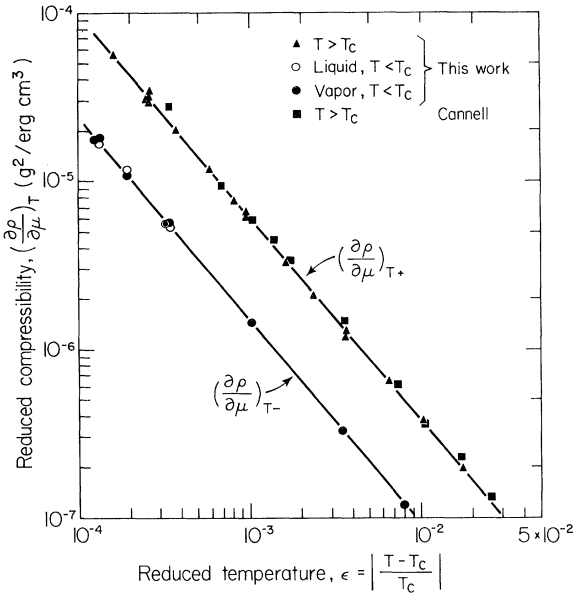

FIG. 1. Reduced compressibility $(\partial\rho/\partial\mu)_{T^+}$ for $T > T_c$ on the critical isochore, and $(\partial\rho/\partial\mu)_{T^-}$ for $T < T_c$ on the coexistence curve, in xenon. The solid lines are best fits by a power-law dependence for ϵ: $(\partial\rho/\partial\mu)_{T^+} = 1.43 \times 10^{-9}\epsilon^{-1.21}$ g²/erg cm³ and $(\partial\rho/\partial\mu)_{T^-} = 0.346 \times 10^{-9}\epsilon^{-1.21}$ g²/erg cm³.

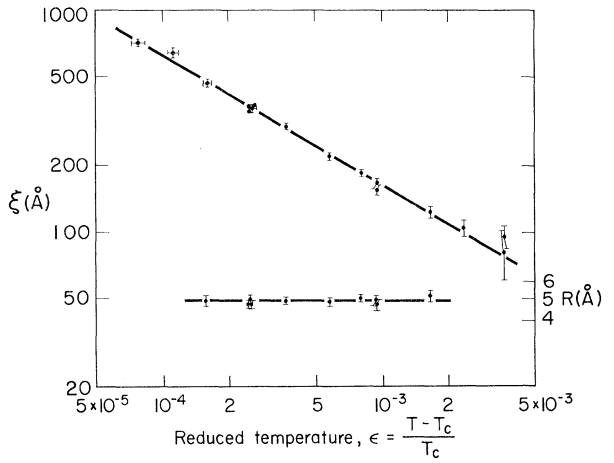

FIG. 2. Long-range Ornstein-Zernike correlation length ξ and short-range correlation length R on the critical isochore in xenon. The solid lines are $\xi = 3.00 \times \epsilon^{-0.58}$ and $R = 4.9$ Å.

along the vapor side of the coexistence curve in the temperature range $0.036°C < T_c - T < 2.3°C$. These results indicate that critical exponents γ and γ' which describe the divergences of $(\partial\rho/\partial\mu)_{T+}$ and $(\partial\rho/\partial\mu)_{T-}$, respectively, are equal within experimental error. Our value of $\gamma = 1.21 \pm 0.03$ is in very good agreement with the value 1.22 ± 0.01 found in CO_2 by Cannell and Lunacek.[6] Our data indicate that $(\partial\rho/\partial\mu)_{T+}/(\partial\rho/\partial\mu)_{T-}$ is equal to 4.1 ± 0.2. According to the van der Waals equation this ratio should equal 2.0. On the other hand, the parametric representation of the equation of state[2] predicts that this ratio is equal to $(\gamma/\beta)[(1-2\beta)\gamma/2\beta(\gamma-1)]^{\gamma-1}$, where β is the exponent that describes the shape of the coexistence curve. Using $\beta = 0.35 \pm 0.02$, obtained from the data of Weinberger and Schneider[7] and our value of γ, we find that $[(\partial\rho/\partial\mu)_{T+}/(\partial\rho/\partial\mu)_{T-}]_{\text{theor}} = 4.2 \pm 0.5$, which agrees well with our experimental result. Our result for $(\partial\rho/\partial\mu)_{T-}$ has the same exponent, within experimental error, as that reported by Giglio and Benedek.[1] However, the numerical values we find for $(\partial\rho/\partial\mu)_T$ in Eq. (3) are 1.6 times those reported in Ref. 1. We believe that the present result is the correct one and represents a much better measurement of the geometrical factors L and Ω. Also, our direct measurement of $(\partial\rho/\partial\mu)_{T+}$ is only 10% different in magnitude from the values deduced rather indirectly from an elaborate and complex analysis of the Brillouin spectra of xenon.[8]

In Fig. 2 we show a graph of our measured values of ξ versus temperature along the critical isochore. These results can be represented by the equation

$$\xi = (3.0 \pm 0.1)\epsilon^{0.58 \pm 0.05}\ \text{Å} \qquad (4)$$

over the temperature range $0.022°C \leq T - T_c < 1.06°C$. We also measured ξ at several temperatures on both the vapor and the liquid sides of the coexistence curve and found good agreement with the previous measurements of Giglio and Benedek.[1] In Fig. 2 we also show values of the direct correlation range R along the critical isochore computed from our measurements of $(\partial\rho/\partial\mu)_{T+}$ and ξ and from the Ornstein-Zernike relation

$$\xi^2/R^2 = (\partial\rho/\partial\mu)_T(\rho^2\kappa_I)^{-1}. \qquad (5)$$

κ_I is the compressibility of an ideal gas at the number density ρ_N, i.e., $\kappa_I = 1/\rho_N k_B T$. Within the experimental error, R appears to be constant and equal to 4.9 ± 0.1 Å. With this value of R we find that the values of ξ computed from Cannell's data on the Brillouin spectrum of xenon are in agreement with the present measurements of ξ. Below T_c we find that ξ may be several percent *larger* in the liquid phase than in the vapor phase at the same temperature, thus suggesting that R may be density dependent.

Using the scaling-law equality $3\gamma'/(2\beta+\gamma') = 2 - \eta$ and the values of γ' and β given above gives $\eta = 0.10 \pm 0.04$. The Josephson inequality $3\nu > 2 - \alpha$ suggests $\alpha \geq 0.26 \pm 0.15$, which is just barely consistent with the value $0 < \alpha < +0.125$ obtained by Edwards, Lipa, and Buckingham[9] who measured the specific heat C_v of xenon. Both inequalities suggest that the value of ν consistent with these inequalities is probably in the upper part of the range we give.

According to the Kawasaki-Kadanoff-Swift (KKS) mode-mode coupling theories,[10,11] the critical part of the thermal diffusivity in the hydrodynamic regime ($q\xi \ll 1$) is related to the Ornstein-Zernike long-range correlation length ξ by the equation

$$(\Lambda/\rho C_p)_{\text{theor}} = k_B T/6\pi\eta\xi. \quad (6)$$

Here Λ is the thermal conductivity, C_p is the specific heat at constant pressure, and η is the shear viscosity which varies quite slowly near T_c. Its magnitude at ρ_c and T_c has been recently measured[12,13] from the spectrum of light scattered from thermally excited surface waves to be $\eta = 495 \pm 12$ μP. We can extend our determination of ξ into the temperature region $1°\text{C} < T - T_c < 4°\text{C}$ by (a) using Eq. (5), taking $R = 4.9$ Å = const; (b) using Eq. (5) with Cannell's Brillouin-scattering data[8] for $(\partial\rho/\partial\mu)_T$, taking $R = 4.9$ Å = const; or (c) graphically extrapolating our direct measurements. These three methods agree within 15% at worst. Using this extrapolation procedure and the above value for the viscosity η, we have calculated the magnitude and temperature dependence of Eq. (6) and have shown the results as a dashed curve in Fig. 3 over the temperature range $0 < T - T_c < 4°\text{C}$. We indicate with vertical bars our estimate of the uncertainty in this procedure. We also show in Fig. 3 the experimentally measured thermal diffusivity as determined by analyzing the data of Henry, Swinney, and Cummins[14] for the spectral width of the quasi-elastically scattered light for scattering angles and the temperatures such that $q\xi \ll 1$.

This figure shows quite clearly that the KKS theory is by no means equal to the experimentally observed result, as had been assumed.[14] An additional contribution to the thermal diffusivity comes from the nondivergent or background thermal conductivity Λ_B. Using the recent data of Tufeu, le Neindre, and Vodar[15] for Λ_B as analyzed by Sengers,[16] we have computed $\Lambda_B/\rho C_p$ using $C_p = C_v + T(\partial P/\partial T)_v^2 \rho^{-3}$ with C_v from the data of Edwards, Lipa, and Buckingham.[9] We have

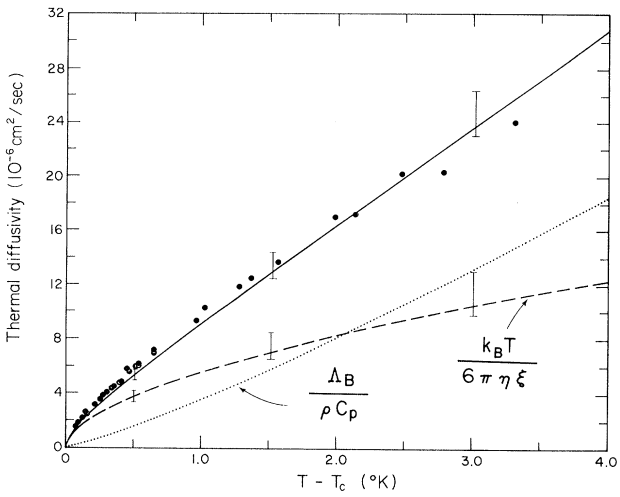

FIG. 3. Thermal diffusivity on the critical isochore in the hydrodynamic limit $q\xi \ll 1$ in xenon. The dashed line is the Kawasaki theretical "critical" contribution, the dotted line is the background contribution, and the solid line is their sum. The solid points represent the measurements of Henry, Cummins, and Swinney, Ref. 14.

taken $(\partial P/\partial T)_v = 1.187$ atm/°C = const for $0 < T - T_c < 4°\text{C}$.[17] The result is shown as a dotted line in Fig. 3. Clearly the background thermal conductivity makes an important contribution to the linewidth as has already been suggested by Sengers and Keyes.[18] The sum $\Lambda_B/\rho C_p + k_B T/6\pi\eta\xi$ is indicated by the solid line and is seen to be in good agreement with the experimentally observed thermal diffusivity.

We would like to express our gratitude to Mr. G. Hawkins and Mr. G. Feke for their collaboration in the comparison of the KKS theories with experiment, and to Professor Swinney for making available to us the Rayleigh linewidth data.

*Research supported with funds provided by the Advanced Research Projects Agency under Contract No. SD-90 with the Massachusetts Institute of Technology.

†Fanny and John Hertz Foundation Fellow.

‡Present address: Centro Informazioni Studi Esperienze, Caselle Postale 3986, 20100 Milano, Italy.

[1]M. Giglio and G. B. Benedek, Phys. Rev. Lett. 23, 1145 (1969).

[2]P. Schofield, J. D. Litster, and J. T. Ho, Phys. Rev. Lett. 23, 1098 (1969).

[3]A. Einstein, Ann. Phys. (Leipzig) 33, 1275 (1910).

[4]L. S. Ornstein and F. Zernike, Proc. Acad. Sci., Amsterdam 17, 793 (1914), and Z. Phy. 19, 134 (1918).

[5]J. A. Chapman, P. C. Finnimore, and B. L. Smith, Phys. Rev. Lett. 21, 1306 (1968).

[6]J. H. Lunacek and D. S. Cannell, Phys. Rev. Lett. 27, 841 (1971).

[7]M. A. Weinberger and W. G. Schneider, Can. J. Chem. 30, 422 (1952).
[8]D. S. Cannell and G. B. Benedek, Phys. Rev. Lett. 25, 1157 (1970); D. S. Cannell, Ph.D. thesis, Massachusetts Institute of Technology, 1970 (unpublished).
[9]C. Edwards, J. A. Lipa, and M. J. Buckingham, Phys. Rev. Lett. 20, 496 (1968).
[10]K. Kawasaki, Phys. Lett. 30A, 325 (1969), and Phys. Rev. A 1, 1750 (1970).
[11]L. P. Kadanoff and J. Swift, Phys. Rev. 166, 89 (1968).
[12]J. Zollweg, G. Hawkins, I. W. Smith, M. Giglio, and G. Benedek, in Proceedings of the Colloque International du Centre National de la Recherche Scientifique sur la Diffusion de la Lumière par des Fluids, Paris, 1971 (to be published).
[13]J. Zollweg, G. Hawkins, and G. B. Benedek, Phys. Rev. Lett. 27, 1182 (1971).
[14]D. H. Henry, H. L. Swinney, and H. Z. Cummins, Phys. Rev. Lett. 25, 1170 (1970), and private communication.
[15]R. Tufeu, B. le Neindre, and B. Vodar, private communication with J. V. Sengers.
[16]J. V. Sengers, private communication.
[17]H. W. Habgood and W. G. Schneider, Can. J. Chem. 32, 98 (1954).
[18]J. V. Sengers and P. H. Keyes, Phys. Rev. Lett. 26, 70 (1971).

Photoemission Measurements of the Valence Levels of Amorphous SiO_2 †

T. H. DiStefano and D. E. Eastman
IBM Thomas J. Watson Research Center, Yorktown Heights, New York 10598
(Received 29 September 1971)

The complete valence band in amorphous SiO_2 has been examined by photoelectron spectroscopy at photon energies of 21.2, 26.9, 40.8, and 1486.6 eV. The spectra show emission from an 11.2-eV-wide p-derived valence band and from the oxygen 2s level at 20.2 eV below the valence-band edge. Four pieces of structure in the p bands are related to the single bonding and the two nonbonding orbitals of the O^{--} ion. A narrow, nonbonding level found at the valence-band edge may cause lattice trapping of valence-band holes.

Amorphous SiO_2 is of considerable technological and theoretical interest, although little is known about the electronic structure of the material. A knowledge of the valence-band structure is important to current studies of radiation damage, electronic structure of various defects, and interface properties for amorphous SiO_2. Several recent theoretical calculations[1-3] have contributed to an understanding of SiO_2 in terms of molecular clusters, but large uncertainties remain because such basic parameters as the principal structure and width of the valence band have not been determined experimentally. Optical measurements[4-6] have fixed the band gap at about 9.0 eV. However, past ultraviolet photoemission studies of wide-gap insulators such as SiO_2 have been limited because of the high photon energy necessary to excite electrons into vacuum. A recent extension of ultraviolet photoemission spectroscopy (UPS) to a photon energy of 40.8 eV has enabled us to probe, for the first time, the entire width of the valence band in amorphous SiO_2.

We present photoelectron spectra from amorphous SiO_2 which display a valence-band width of 11.2 eV and four clearly discernable pieces of structure.[7] The valence band, described in terms of a simple basis of wave functions on the O^{--} ion, comprises one bonding and two nonbonding oxygen orbitals. This identification of valence-band structure is based on UPS, x-ray photoemission spectroscopy (XPS), and soft x-ray spectroscopy (SXS) data. A narrow, nonbonding orbital which lies at the valence-band edge indicates a low hole mobility. Valence-band holes which have been lattice trapped in this narrow band may explain the positive charge induced by ionizing radiation in SiO_2.

The UPS energy distributions were measured by using a cylindrical electrostatic-deflection energy analyzer, with a windowless capillary discharge in He or Ne gas as a light source.[8] Photoemission distributions for $\hbar\omega = 21.2$, 26.9, and 40.8 eV were obtained from a 150-Å film of amorphous SiO_2 which was thermally grown on (100) silicon. Spectra obtained from sputter-deposited films of amorphous SiO_2 were essentially identical to those from the oxidized silicon. During the measurements, care was taken to minimize charging of the insulating samples. The salient features in the UPS measurements were found to be insensitive to vacuum conditions.

Several emission spectra for amorphous SiO_2